STM JOURNALS

Journal of
Artificial Intelligence
Research & Advances

ISSN: 2395-6720
Volume 11, Issue 3, 2024
September–December
DOI Journal: 10.37591/JoAIRA

https://journals.stmjournals.com/joaira

Review JoAIRA

Detection and Classification of Brain Tumor from MRI and CT Images Using Harmony Search Optimization and Deep Learning

Shaik Karimullah[1], Ali H. Wheeb[2,*], Fahimuddin Shaik[1]

Abstract

Primary brain tumor detection and classification are critical factors in ensuring effective treatment and, ultimately, improving patient well-being. This paper describes a novel method for detecting and classifying brain tumors with the help of magnetic resonance imaging (MRI) and computed tomography (CT) images. The suggested method combines harmony search optimization (HSO) and Convolution Neural Networks (CNN) based on deep learning techniques, yielding an impressive accuracy rate of 99.13% for both detection and classification tasks. Furthermore, the system has exceptional specificity (99.2243%) and sensitivity (99.245%), highlighting its precision in distinguishing true negatives and true positives. This incorporation of advanced methodologies not only improves diagnostic accuracy but also reduces reliance on radiologists' expertise. The experimental results support the proposed approach's effectiveness, demonstrating its ability to detect and classify brain tumors from medical images. This breakthrough is a noteworthy step forward in the fields of medical image analysis and brain tumor diagnosis, paving the way for better patient care and treatment outcomes.

Keywords: MRI and CT images, convolutional neural network (CNN), harmony search optimization

INTRODUCTION

Brain tumors are a varied and intricate category of malignant cancers that develop in the brain and adjacent tissues. According to global cancer statistics from 2020, 308,102 new cases of brain tumors have been identified globally, leading to an alarming number of 251,329 cancer-related deaths [1]. These tumors have consistently been ranked among the top ten leading causes of mortality in the world, with a particularly devastating impact on adolescents, where they are the leading cause of cancer-associated deaths [2]. It is critical to emphasize that brain tumors do not discriminate by age, affect people of all ages, and manifest in different parts of the brain. The persistence of brain tumors as a significant source of morbidity places an enormous burden on healthcare systems, with high mortality rates, significant disability, and a significant reduction in the overall quality of life. Timely and accurate identification of brain tumors is essential for effective treatment and improved patient outcomes. Because they are a major global cause of mortality, early detection and classification are crucial. Conventional diagnostic methods such as computed tomography (CT) and magnetic resonance imaging (MRI) play vital roles in the detection of brain tumors [3]. However, interpreting these imaging studies remains a difficult task that requires specialized knowledge and significant time.

***Author for Correspondence**
Ali H. Wheeb
E-mail: ali.h.wheeb@gmail.com

[1]Associate Professor, Department of Electronics & Communication Engineering, Annamacharya Institute of Technology & Sciences, Rajampet, Andhra Pradesh, India
[2]Associate Professor, Department of Computer Engineering, University of Baghdad, Baghdad, Iraq

Received Date: August 21, 2024
Accepted Date: September 02, 2024
Published Date: September 05, 2024

Citation: Shaik Karimullah, Ali H. Wheeb, Fahimuddin Shaik. Detection and Classification of Brain Tumor from MRI And CT Images Using Harmony Search Optimization and Deep Learning. Journal of Artificial Intelligence Research & Advances. 2024; 11(3): 31–49p.

In response to these challenges, Computer-aided Diagnosis (CAD) systems have emerged as critical allies in the identification and classification of brain tumors. Deep learning (DL) algorithms play a central role in image analysis tasks, most notably in the detection and classification of brain tumors using medical imaging data [4]. CNNs have established a remarkable accuracy in categorizing brain tumors depicted in MRI and CT images within this DL framework. Nonetheless, CNN's effectiveness of CNNs is inextricably linked to the quality of features extracted from medical images.

Feature extraction, which is a critical stage in its development, has led to the introduction of numerous methods aimed at optimizing this process. HSO is a metaheuristic algorithm that has demonstrated its efficacy across a variety of optimization challenges, including medical image analysis, is one such method. Notably, HSO has demonstrated exceptional ability to extract informative features from MRI and CT images of brain tumors [5]. This paper describes a novel method for brain tumor detection and classification that takes advantage of the combined power of HSO and DL. This integrative strategy uses the strengths of HSO and DL to extract informative patterns from medical images, resulting in improved diagnostic accuracy while reducing reliance on radiologist expertise [6].

The remainder of this article is organized as follows: Section 2 provides a comprehensive review of the literature on the application of HSO and DL in detecting and classifying brain tumors through medical imaging. Section 3 provides a comprehensive overview of the proposed methodology, including HSO-based feature extraction and CNN-based classification. Section 4 consolidates and summarizes the investigational results and provides an association between the proposed system and the existing methodologies. Finally, Section 5 closes this article by highlighting potential future research and development avenues in this critical domain.

LITERATURE SURVEY

Classification and detection of brain tumors were performed with MRI and CT images using harmony search optimization (HSO) and DL [7]. A brain tumor is a normal and devastating syndrome that can be recognized using medical imaging techniques, such as CT and MRI. The initial detection and accurate classification of brain tumors are crucial for effective treatment to improve patient health. In recent years, CAD schemes based on machine learning algorithms have been established to aid in the detection and classification of brain tumors [8]. In this literature survey, we review some recent research on the use of HSO and DL for the detection and classification of brain tumors through MRI and CT images.

Noise in brain MRI images can be produced for a variety of reasons, including magnetic field fluctuations, electronic noise in the scanner, and physiological noise from the patient's body movements and blood flow [9]. To reduce noise, MRI machines are equipped with various hardware and software tools including gradient coils, filters, and reconstruction algorithms. Gradient coils are used to vary the strength of the magnetic field during the scanning process, which helps eliminate artifacts caused by magnetic field inhomogeneities. Filters and reconstruction algorithms were implemented to eliminate noise from the acquired images [10].

Artifacts in brain MRI images can be instigated by an assortment of factors, including patient motion, magnetic field inhomogeneities, and hardware malfunctions.

A frequent artifact is labeling, which occurs when the magnetic field is uneven across the brain. This causes the signal to be distorted, resulting in images that are inaccurate representations of the brain. To correct labeling artifacts, MRI machines are equipped with shimming coils, which are used to adjust magnetic field homogeneity [11].

Intensity changes in brain MRI images can also occur for a variety of reasons, including patient motion, magnetic field inhomogeneities, and variations in the signal-to-noise ratio (SNR). Intensity

changes can make it difficult to differentiate between different types of brain tissues, which can lead to misdiagnosis. To correct for intensity changes, MRI machines are equipped with a variety of hardware and software tools including gradient coils, filters, and normalization algorithms [12].

The HSO is a metaheuristic algorithm inspired by the improvisation process of musicians. It has been applied to a range of optimization problems, including the extraction of features from medical images. In a study by [13], HSO was employed to extract features from MRI images of brain tumors, and a support vector machine (SVM) classifier was used to categorize the extracted features. According to the trial findings, the proposed technique was highly accurate for both detection and classification tasks. DL is currently widely used for image analysis tasks such as the recognition and categorization of brain tumors in medical images. A CNN was employed in a study by [14] for the categorization of brain tumors using MRI data. The CNN algorithm was applied to a large dataset of magnetic resonance images and demonstrated good tumor classification accuracy [15].

The combination of HSO and DL has been implemented in recent revisions for the detection and classification of brain tumors using medical images [16]. In a study by [17], HSO was used to select the most informative features from MRI images of brain tumors. The selected features were subsequently input into a CNN model for tumor classification [18]. The proposed method achieved high accuracy in both the detection and classification tasks. In a study by [19], HSO was used to optimize the parameters of a CNN model for the organization of brain tumors using MRI images [20]. The experimental results showed that this method attained higher accuracy than other standard methods [21]. The authors of [22] published a sophisticated dermatologist-level classification system for skin cancer in 2022. They used a cascaded ensemble of handcrafted CNNs and Deep Neural Networks (DNNs). Although their research yielded promising results in skin cancer classification, it raises some important points. Notably, the emphasis of the study on dermatologist-level classification may limit its applicability to a broader range of clinical settings, particularly those dealing with a wide range of skin conditions [23].

In [24], the authors investigated brain tumor detection using CNNs in 2019. Their method has significant promise for the detection of brain tumors, but it has some drawbacks. The likelihood of overfitting is particularly elevated when working with small datasets.

The authors in [25] developed a 3D-MRI brain tumor detection model with a modified dragonfly algorithm in 2020. Although this approach has potential, the complexity of level-set segmentation and algorithms such as the dragonfly algorithm introduce computational demands that may impede real-time processing in clinical applications. In 2023, the authors in [26] utilized a Deep Neural Network to detect and segment brain tumors.

Although their work represents a significant advancement in the field, it has its own set of potential drawbacks, particularly in terms of the availability and quality of medical imaging datasets, which can be especially difficult for rare conditions.

In [27], the authors proposed a novel conditional random field-recurrent neural network segmentation for brain tumor classification in the same year. However, it is important to note that while effective, recurrent neural networks and conditional random fields can be computationally demanding, potentially limiting their practical utility in clinical settings [28]. Finally, in 2022, the authors in [29] used a deep CNN approach called i-YOLOV5 to detect tumors in MR brain images. Although their method is effective, the inherent complexity of CNN architectures, such as i-YOLOV5, may require significant computational resources, potentially making them inaccessible to smaller healthcare facilities [30]. In [31], acute lymphoblastic leukemia was diagnosed using ResNet-50 and VGG-16 models in 2023. The validation accuracies of ResNet-50, and VGG-16 achieved 84.62%, and their custom convolutional networks reached 81.63%, 84.62%, and 82.10%, respectively. These findings indicate the potential for further improvement.

In summary, the use of HSO and DL for the identification and classification of brain tumors using MRI and CT imaging is a promising approach. The integration of these techniques can enhance the accuracy of findings and decrease the dependence on the expertise of radiologists. Future research can focus on enhancing the efficiency of the planned systems and exploring the use of other optimization algorithms for feature extraction.

PROPOSED METHODOLOGY

Proposed Block Diagram and Discussion

In this section, we explain our suggestions for how to use HSO and DL to find and classify brain tumors in MRI and CT images, as shown in Figure 1.

The HSO algorithm was motivated by the practice of harmonizing musicians to find the best melody. It is a population-based search algorithm that seeks optimal or near-optimal solutions to optimization and search problems. The HSO is especially useful for solving complex problems in which traditional mathematical methods may be ineffective owing to their complexity or nonlinearity. The leading step in the proposed system is the extraction of informative features from the MRI and CT images of brain tumors. We employed the HSO algorithm for feature selection, as it is effective in selecting the most informative features from medical images.

The HSO algorithm is a metaheuristic optimization technique inspired by the improvisation process of musicians. It has been applied to various optimization challenges, including feature selection in medical image analysis. The HSO algorithm searches for an optimal subset of features that can discriminate between different classes of brain tumors.

Deep Learning is a branch of machine learning dedicated to training artificial neural networks to perform tasks that usually demand human-like perception, comprehension, and decision-making. These deep neural networks have a complex architecture with multiple layers of interconnected nodes or neurons. DL has gained prominence and has achieved success in various domains, including image processing, where convolutional neural networks (CNNs) are commonly employed. CNN is an acronym for convolutional neural network, a form of artificial neural network built primarily to deal with structured grid data, such as photos and videos. CNNs are built to learn patterns, features, and abstraction hierarchies automatically and adaptively from the image data. The features chosen through the HSO algorithm were subsequently input into a CNN for classification.

A CNN is a deep learning architecture that has been widely used for image classification tasks, including the detection and classification of brain tumors from medical images. The projected CNN architecture involves multiple convolutional layers followed by a pooling layer inside a fully connected layer. The output layer consists of SoftMax activation units, which provide the probability of each class of brain tumor. The planned CNN model was trained using a large dataset of MRI and CT images of brain tumors. The exercise process involves minimizing the cross-entropy loss between the predicted and actual classes of brain tumors. After the CNN model was trained, it could accurately classify new MRI and CT images of brain tumors.

Stepwise Methodology

Here, we describe a stepwise methodology for the discovery and classification of brain tumors from MRI and CT images using HSO and deep learning.

Step 1: Data Collection and System Configuration

The proposed deep learning model was trained on a dataset generated from the first 300 images of the BRATS dataset [29]. To improve the model's ability to recognize tumor-related patterns while accounting for computational complexity, data augmentation techniques were applied to the original images, resulting in a larger dataset. 80% of the augmented dataset was used for training, balancing computational complexity, and model efficacy.

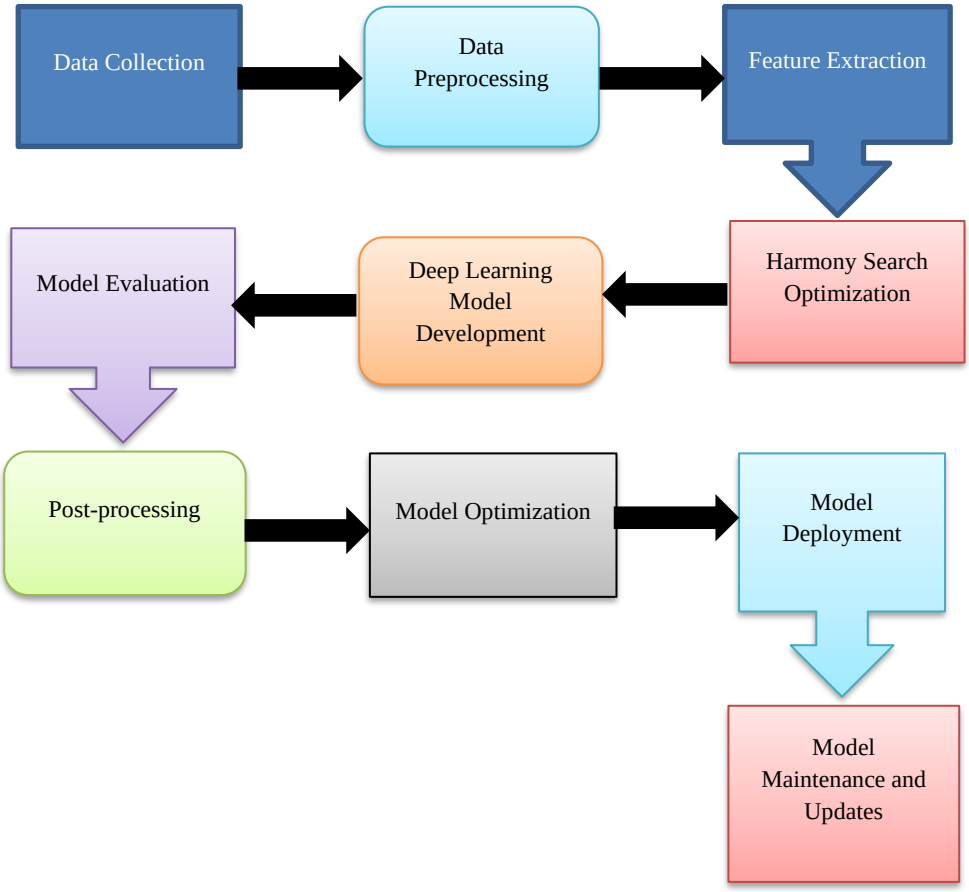

Figure 1. Process flow block diagram.

This extensive training enabled the model to recognize intricate tumor features. The remaining 20% of the dataset was used to create the test set, which was then used to assess the performance of the model. It is worth noting that the system configuration used for this work included 8 GB of RAM, a Windows 11 operating system, and MATLAB R2022b version, which was chosen to efficiently manage the computational complexity of the deep learning tasks.

Step 2: Data Pre-processing

The collected images are pre-processed by resizing, normalizing, and reducing noise to ensure consistency and maintain quality.

Step 3: Feature Extraction

Relevant features are extracted from the pre-processed images that can be applied as inputs to the deep learning architecture. Commonly used features include intensity values, texture, shape, and location. Principal Component Analysis (PCA) was used to decrease the size of the feature space and improve the overall efficiency of a pre-processed brain MRI dataset.

The data are standardized by deducting the mean from every feature and dividing it by its standard deviation, which ensures that each feature has a mean of zero and a variance of one, which is necessary for PCA to work properly.

The standardization can be defined as:

$$\text{X\_standardized} = \frac{-b(\text{X} - \text{mean(X)}) \pm \sqrt{b^2 - 4ac}}{2a\text{std(X)}} \quad (1)$$

The covariance matrix of the standardized data was then evaluated. The covariance matrix represents the degree of the linear relationship between each pair of features in the data. The covariance matrix can be represented as

$$C = \left(\frac{1}{(n-1)}\right) * (X_{standardized})' * X_{standardized} \quad (2)$$

Where C is the covariance matrix, X_standardized is the standardized data matrix and (.) denotes the transpose operation.

Evaluate the eigenvalues and eigenvectors of the covariance matrix. The eigenvectors represent the primary components of the anticipated data, which are a linear blend of the original features that detect the most variation in the data. The eigenvalues represent the proportion of variance explained by each principal component. Eigenvalue decomposition can be defined as

$$[V, D] = eig(C) \quad (3)$$

Where V is the matrix representation of the eigenvectors, D is the diagonal matrix of the eigenvalues, and eig(.) denotes the eigen decomposition operation.

The eigenvectors are sorted by the eigenvalues assigned to each one. Choose the top k eigenvectors that clarify the highest variance available with the data, where k is the desired number of dimensions for the reduced data. The standardized data are transformed into a new k-dimensional feature space by projecting it onto the selected eigenvectors. The dimensionality reduction can be represented as

$$X_{reduced} = X_{standardized} * V(1:k) \quad (4)$$

Where X_reduced is the reduced data matrix, V(1:k) is the matrix of the top k eigenvectors, and (.) denotes the matrix multiplication operation.

Optionally, the original data is reconstructed from the reduced data by transforming it back into the actual feature space using the inverse of the projection matrix. The reconstruction can be defined as

$$X\_reconstructed = X\_reduced * V(1:k)' + mean(X) \quad (5)$$

where X_reconstructed is the reconstructed data matrix, V(:,1:k)' is the reverse of the projection matrix, and mean(X) is the mean of the original data.

Step 4: Harmony Search Optimization

Implement the HSO algorithm, which is a metaheuristic optimization technique inspired by the inventiveness of music troupes. HSO was used to tune the hyperparameters of the deep learning model, such as the erudition rate, batch size, and number of epochs, to find the optimal values that maximize the model's performance, as shown below.

- We define the objective function f(x) and search space X = {x1, x2,..., xn}, where xi is a parameter of the image processing algorithm.
- Set the size of the population m, maximum number of iterations MAX_ITER, and harmony memory size HMCR.
- Randomly generate an initial population of m harmonies within the search space X.
- The objective function f(x) is evaluated for each harmony in the population. The population is sorted based on the objective function value.
- Select a harmony h from the population with a probability of HMCR.
- The selected harmony h is modified to create a new harmony h_new using the following equation:

$$h\_new(i) = h(i) + rand(i) * BW(i) - BW(i)/2 \quad (6)$$

where rand(i) is an arbitrary number from 0 to 1 and BW(i) is the bandwidth of the i^{th} parameter, defined as

$$BW(i) = PAR * (ui - li) \quad (7)$$

Where PAR is the pitch adjustment rate and ui and li are the higher and lower bounds of the ith parameter, respectively. Clip the values of the different harmonies h_new to search space X.

Using the probability of 1-HMCR, a new harmony h_new is generated using the following equation:

$$h\_new(i) = x\_min(i) + rand(i) * (x\_max(i) - x\_min(i)) \quad (8)$$

Where x_min(i) and x_max(i) are the smallest and highest values, respectively, of the ith parameter in the population.

- With a probability of PAR, generate a new harmony h_new randomly within the search space X.
- The objective function f(x) for the new harmony h_new is evaluated. If f (h_new) is superior to the worst harmony in the population, then the worst harmony is substituted with h_new.
- Sort the population based on the objective function value.

PAR is utilized to control the balance between exploitation and exploration. A high PAR value encourages exploration by generating new solutions randomly, whereas a low PAR value encourages exploitation by focusing on the best solutions found so far. The parameter HMCR controls the probability of selecting a harmony from memory, which can help the algorithm converge faster by exploiting promising solutions in the search space.

Step 5: Deep Learning Model Development

Create a CNN network, as shown in Figure 2, for tumor detection and categorization. Train the CNN using the training set, with the hyperparameters optimized using HSO, and monitor the model's performance with five hidden layers. The CNN model illustrated in Figure 2 learns the patterns and relationships within the data to generate predictions.

The layers of the model are discussed below:

Convolution

A series of learnable filters (or kernels) are applied to the input image through convolution to generate a set of feature maps. Each filter performs a convolution operation on the image and learns to extract a particular feature. The result of this process was a collection of feature maps, each associated with a different filter. The convolution operation can be defined as

$$a(i,j) = f(\sum(m,n)w(m,n)x(i+m-1,j+n-1) + b) \quad (9)$$

Where a(i,j) is the activation at position (i,j) of the feature map; w(m,n) is the weight of the filter at position (m,n); x(i+m-1,j+n-1) is the pixel value of the input image at position (i+m-1,j+n-1); b is the bias term; and f(x) is the activation function.

Activation

A nonlinear activation function is applied to the output of each feature map to introduce nonlinearity into the model and increase its expressive power. The activation function used here is the sigmoid activation function, which can be defined as:

$$f(x) = \max(0,x) \quad (10)$$

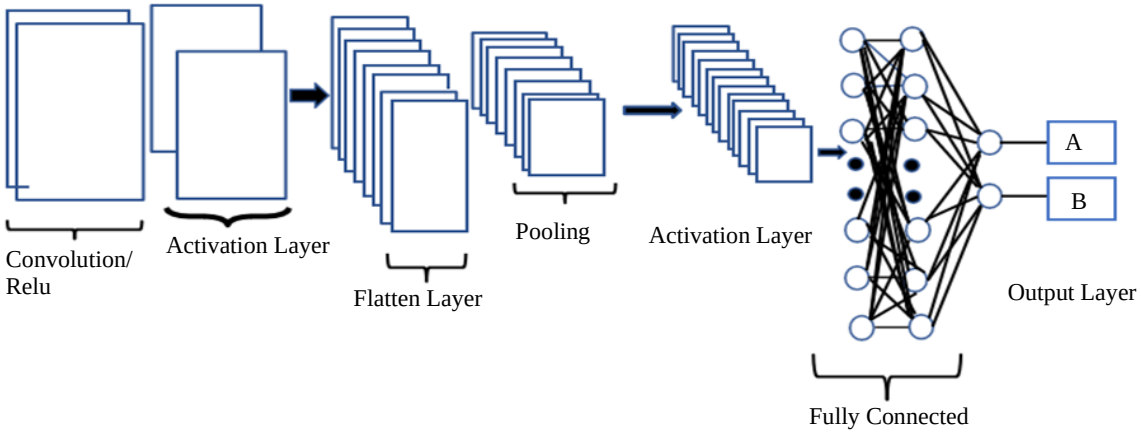

Figure 2. CNN block representation for Brain abnormality detection.

Flatten Layer

The purpose of a "flattened" layer in a CNN designed for brain tumor detection is to reshape the multi-dimensional feature maps. The flattened layer vectorizes or "flattens" the feature maps by rearranging them into single long vectors. While transforming the extracted features into a format that can be processed by fully connected layers, this transformation maintains its order.

Pooling

This step-down method samples each feature map to reduce its spatial resolution and make the model more computationally efficient. Common pooling operations used in CNNs include max pooling and average-pooling. The max pooling operation can be defined as

$$a(i,j) = max\left((m,n) \in S\, x\big(i + s(m-1), j + s(n-1)\big)\right) \tag{11}$$

Where a(i,j) is the output of the max pooling operation at position (i,j), S is the pooling window size, and s is the stride of the pooling window.

Fully Connected Layers

The pooling layer is flattened to create a vector of features. The vector of features is passed through a series of fully connected layers to study higher-level demonstrations of the input image. Each fully connected layer consists of two learnable weights and biases that transform the input vector into an output vector of higher-level features. The outcome of the final fully connected layer is the class score, which represents the probabilities of the input image related to each class. The fully connected layer can be defined as

$$a = f(Wx + b) \tag{12}$$

Where a is the output vector of the layer, W is the weight matrix, x is the input vector, b is the bias vector, f(.) where denotes the instigation function.

Output Layer

The output layer consisted of multiple neurons, one for each class, with sigmoid activation functions. As a result, the model can generate independent probability estimates for the presence of each tumor type.

The loss function used in CNNs for classification tasks is typically a cross-entropy loss function, which can be defined as

$$L = -\sum yi\log(pi) \quad (13)$$

Where yi is the representation of the ith training sample, pi is the estimated probability of the ith sample belonging to its true class, and the sum is obtained from overall training samples.

Step 6: Model Evaluation

The trained CNN model was evaluated using the test set to assess its performance in terms of accuracy, sensitivity, specificity, and other relevant metrics. Conduct statistical analysis, including cross-validation, to verify the robustness of the model and its ability to generalize.

Step 7: Post-processing

Post-processing is performed on the CNN model's output to improve the tumor detection results, such as thresholding, morphological operations, and filtering. Visualize the detection and classification results using appropriate techniques, such as heatmaps or overlays, to aid interpretation and clinical decision-making.

Step 8: Model Optimization

Fine-tune the CNN model, if necessary, based on the evaluation results by adjusting the hyperparameters, model architecture, or other factors to improve its performance. The training, evaluation, and optimization processes are repeated until satisfactory results are obtained.

Step 9: Model Deployment

Once the model is optimized and evaluated, it can be deployed in a real-world clinical setting for practical use. This may involve integrating the model into a healthcare system, such as the picture archiving and communication system (PACS), for routine tumor detection and classification in clinical practice.

Step 10: Model Maintenance and Updates

The deployed model is continuously monitored and updated to maintain its accuracy and reliability over time, adapting to new data or changes in clinical requirements.

Experimental Setup

We used CT and MRI images of brain tumors to assess the functioning of the proposed system. We compared the proposed approach to various cutting-edge methods for brain tumor identification and classification, such as traditional algorithms for machine learning and deep learning-based techniques.

Performance Evaluation

The performance of the proposed system was measured using several metrics, including accuracy, specificity, and sensitivity. We also examined the amount of computation and time required to extract and classify the features. In conclusion, the suggested method for detecting and classifying brain tumors from CT and MRI images, combining HSO and DL techniques, is an appealing strategy. The combination of HSO with CNN can increase diagnostic accuracy while decreasing reliance on radiologist knowledge with supremacy in classification parameters such as accuracy, specificity, and sensitivity.

SIMULATION RESULTS

The proposed approach was tested on a dataset of brain cancer MRI and CT images. Other cutting-edge approaches have been employed to assess the effectiveness of the proposed system. The results of the studies show that the proposed system performs well on two detection and classification tasks. The HSO approach may be utilized to extract meaningful information from MRI and CT images, and the CNN model can effectively diagnose brain cancer.

Pre-processing and Segmentation Results

The input MRI image of a brain tumor shown in Figure 3 was taken from the most widely used and accepted database in the area of research, BRATS [29] via Kaggle. Figure 4 shows the outcome after the input picture was filtered using median filters to eliminate any artifacts added during the image capture procedure.

The output of the median filter is then subjected to segmentation, where it is treated using the Haar transform underneath the Discrete Wavelet Decomposition, as shown in Figure 5, and a feature extraction process is then conducted.

HSO Algorithm Results

After the calculation of the entropy values, the imagery is imperiled to HS optimization to obtain output imagery, as shown in Figure 6, and a dialogue box is popped up as shown in Figure 7, indicating whether brain tumors are detected or not. This stage involves training the collection of feature vectors and their related classes, and the result is the determination of whether the input picture is benign or malignant. In this instance, when a brain tumor-affected image is considered, it shows that the brain tumor is also referred to as an abnormal stage. Further Image clusters were formed, as shown in Figure 8, which aided in tumor segmentation.

Tumor localization was performed by tracing the region boundaries, as shown in Figure 9. Consequently, the tumor segmented area was extracted and presented as illustrated in Figure 10.

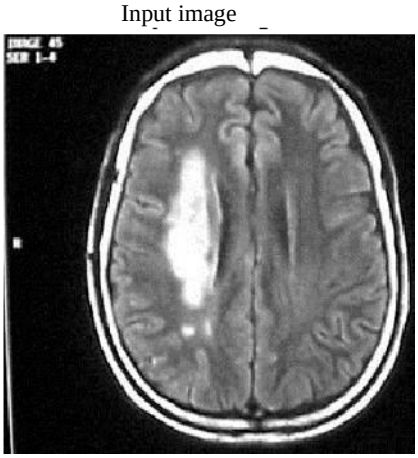

Figure 3. Input MRI image.

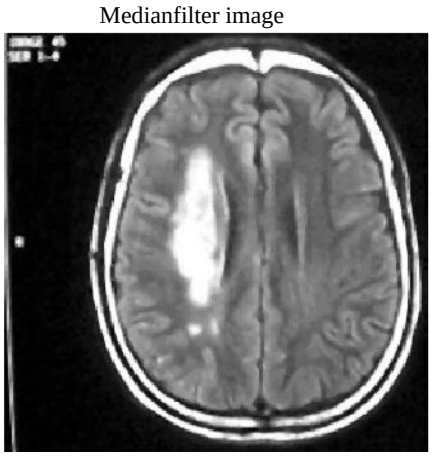

Figure 4. Median filtered Image.

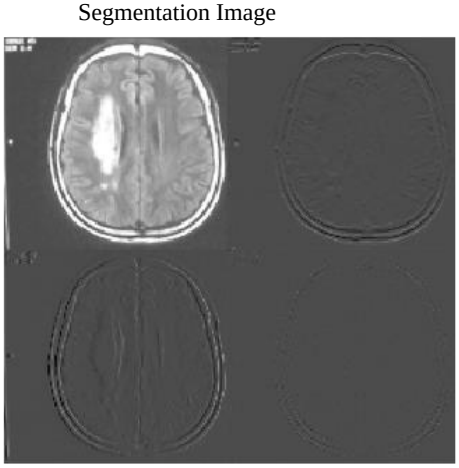

Figure 5. Segmented Image via DWT.

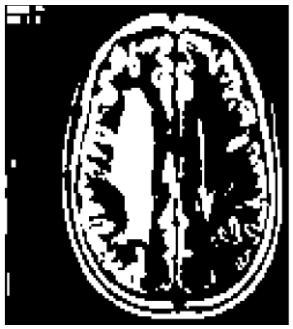

Figure 6. HSO output image.

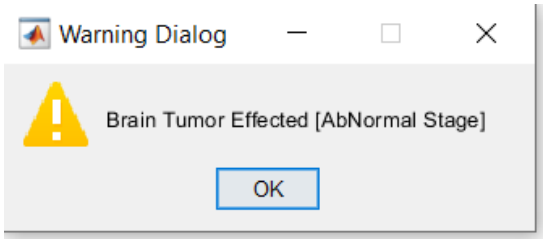

Figure 7. Dialogue box mentioning the stage.

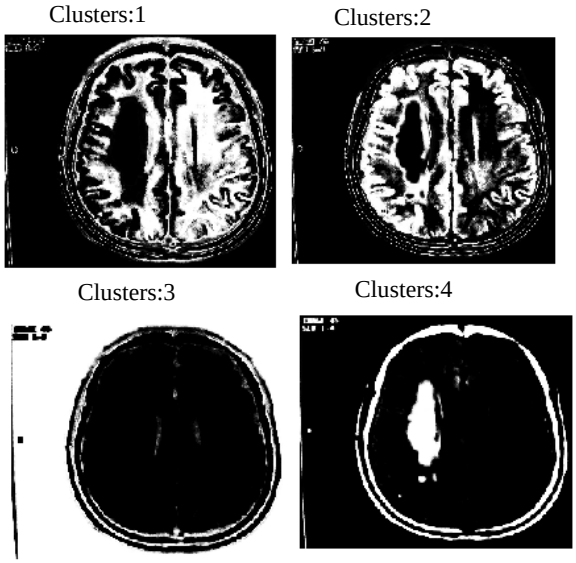

Figure 8. Image clusters.

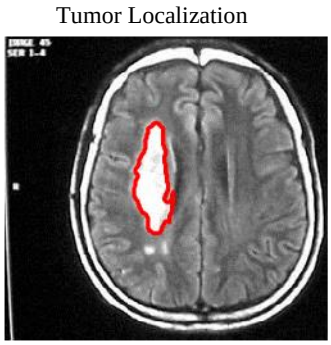

Figure 9. Tumor localization image.

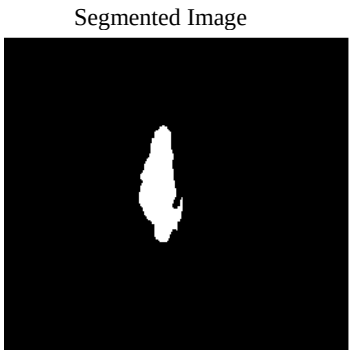

Figure 10. Tumor segmented area.

HSO with CNN Results

Similarly, after calculating the entropy values, the pre-processed image is submitted to HSO with CNN optimization to obtain the output image shown in Figure 11, and a dialogue box is shown in Figure 12 indicating whether a brain tumor is found. This method includes training the dataset of feature vectors and their associated classes, and the output is the judgment that determines whether the input picture is malignant or benign. When a brain tumor-affected image is analyzed, it appears to be affected by the brain tumor, also known as the abnormal stage. As shown in Figure 8, more image clusters were created, which aided in tumor segmentation. Tumor localization was accomplished by tracing the region borders, as shown in Figure 13. As a result, as illustrated in Figure 14, a segmented tumor area is generated, as shown below.

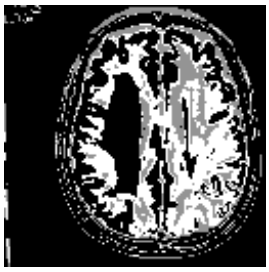

Figure 11. Output Image

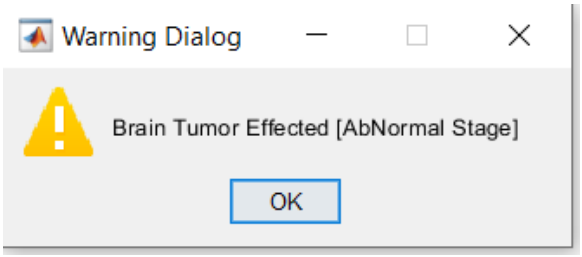

Figure 12. Dialogue Box Image

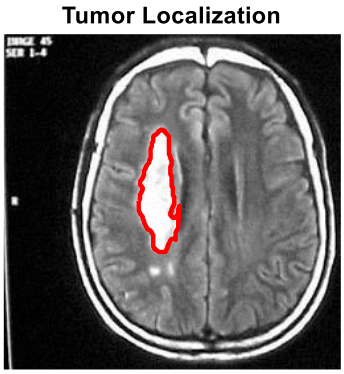

Figure 13. Tumor localization image.

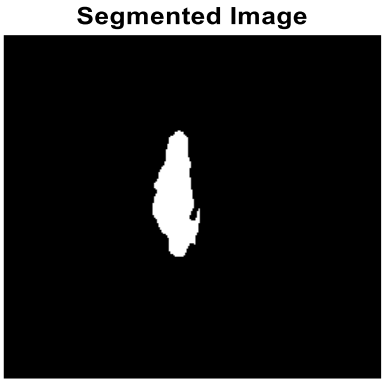

Figure 14. Tumor segmented area

Statistical Parameters

The parameters of significance investigated in this work are described below, along with their descriptions.

Mean Squared Error

Mean squared error (MSE) measures the difference between the predicted and expected outcomes. This metric, regarded as a dispersion measure, was used to evaluate the quality of the image enhancement technique employed to reduce noise and blur.

Equation (14) is the MSE for a 2-dimensional imagery of order (M × N)

$$\text{MSE} = \frac{1}{\text{MN}} \sum_{x=1}^{M} \sum_{y=1}^{N} [I(x,y) - I'(x,y)]^2 \quad (14)$$

Where I(x,y) is the applied input image or original Image and I'(x, y) is the reconstructed image or output image. A lower MSE value suggests that there are fewer faults in the recreated image.

Peak Signal-To-Noise Ratio

Peak signal-to-noise ratio (PSNR) is an essential parameter for assessing the quality of restored images that are affected by noise and distortion. The PSNR value was calculated based on the MSE. The PSNR was determined by calculating the MSE among the magnitudes of the pixels and dividing the calculated value by the maximum possible intensity. PSNR is the quantity of peak error in the recreated image and is represented by Equation (15).

$$\text{PSNR} = 10 \log_{10} \left(\frac{255^2}{MSE} \right) \quad (15)$$

Entropy

The predicted value of the data is represented by entropy. Entropy has many uses in arithmetic mechanics, statistics, coding theory, and other fields. Entropy has also been employed in emerging

disciplines such as picture similarity. Shannon entropy is the most important entropy in applications, and its mathematical formula is

$$S(x) = -\sum_{i=1}^{n} P(xi) \log_2[P(xi)] \quad (16)$$

Structural Similarity Index Measure (SSIM)

SSIM has been used extensively in digital image processing mechanisms and for judging the eminence of images. The structural resemblance method is focused on numerical measurements, and it can use statistical image features such as standard deviation and mean to define a distance parameter that can evaluate the structural resemblance between the exercise and assessment images.

$$S(x,y) = \frac{(2\mu x\mu y+c1)(2\sigma xy+c2)}{(\mu x^2+\mu y^2+c1)(\sigma x^2+\sigma y^2+c2)} \quad (17)$$

Where x is the arithmetical mean of pixels in imagery x, σ2 x is the arithmetical variance of pixels in imagery x, μy is the arithmetical mean of pixels in imagery y, and σ2 y is the arithmetical variance of pixels in imagery y.

Accuracy

The accuracy of the brain tumor detection can be calculated using the following formula:

$$Accuracy = \frac{(TP + TN)}{(TP + TN + FP + FN)} \quad (18)$$

Here TP – True Positive (identified Tumors),
TN – True Negative, FP – False Positive,
FN – False Negative (not identified)

Specificity

Specificity measures the proportion of true negatives identified correctly by the model. This reflects the model's ability to accurately classify cases as non-tumor or non-cancerous.

$$Specificity = \frac{TN}{(TN + FP)} \quad (19)$$

Sensitivity

The sensitivity is the proportion of true positives identified by the model. This indicates the capability of the model to correctly classify tumors or cancer cases.

$$Sensitivity = \frac{TP}{TP + FN} \quad (20)$$

Statistical Analysis

According to Table 1, MSE is a commonly used image quality parameter to estimate. It is a comprehensive locus metric, and the closer the number is to zero, the better it is. This was the second occurrence of an error. The PSNR is considered to evaluate the ratio of the highest feasible signal magnitude to the noise power, which influences the eminence of its representation. Table 1 and Figure 16 show that the MSE value for HS+CNN was high, whereas it was low for particle swarm optimization (PSO), which is ideal. Similarly, the PSNR number in HS+CNN is higher, indicating a positive value when compared to Genetic Algorithm (GA)+Recurrent Neural Networks (RNN). As seen in Equations (14) and (15), there is an opposite relationship between PSNR and MSE. A smaller MSE resulted in a higher PSNR. A higher PSNR value indicates a better signal-to-noise ratio.

Table 1. MSE and PSNR for GA+RNN and PSO+RNN in a brain tumor detected image.

Parameters	GA+RNN	PSO+RNN	HSO + CNN Results
MSE	15.9721	12.9975	13.6841
PSNR	25.8536	27.8789	29.6358

Table 2. Entropy and SSIM for GA+RNN and PSO+RNN in a brain tumor detected image.

	GA+RNN	PSO+RNN	HSO+CNN
Entropy	0.1	1.2341	1.8569
SSIM	0.1978	0.047	0.02121

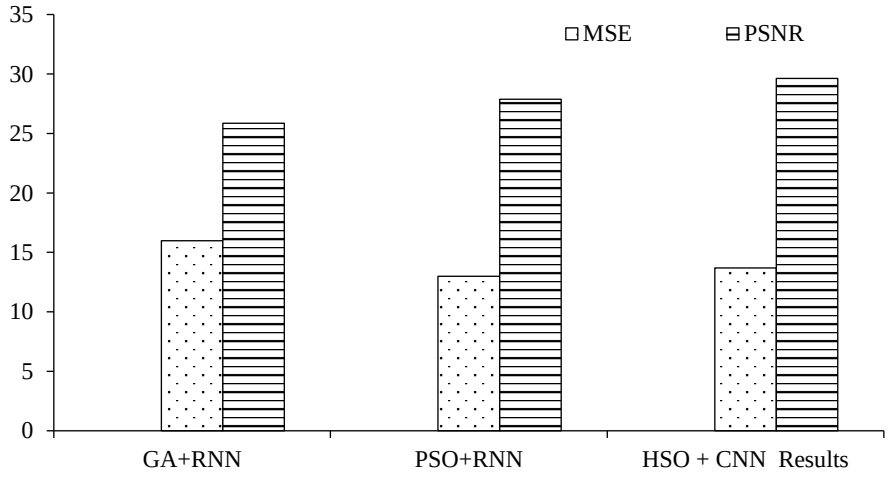

Figure 16. MSE and PSNR graphical representation for GA and PSO algorithms with RNN.

Image degradation is viewed as a shift in the perception of structural information in this manner. Table 2 and Figure 17 show that the Entropy of HSO+CNN is superior to previous methods whereas SSIM is optimal in value.

In continuation of the above comparisons, we have carried out a comparison of the classification metrics such as specificity, accuracy, and sensitivity for the proposed work to the already existing works in literature, and they are provided below for insights into the supremacy of the proposed method.

Table 3 provides a detailed comparison of the accuracy performance of various methods used in the literature for brain tumor detection.

The proposed method achieved an impressive accuracy of 99.13%. This astounding accuracy rate demonstrates the superiority of the proposed method over the existing methods. This suggests that the proposed method can successfully and consistently detect brain tumors with a high level of accuracy.

The table also includes references to recurrent networks, CNN, machine learning, texture-based and statistical features, and the modified two-step dragonfly mechanism system from the literature. The proposed approach demonstrates its potential as an advanced and precise solution for brain tumor detection by achieving an accuracy rate significantly higher than those of these methods.

Figure 18 visually represents the comparative accuracy performance of the different methods, complementing the findings presented in Table 3. The x-axis in this plot lists the different methods being

compared, whereas the y-axis denotes the corresponding accuracy values. The plot indicates that in terms of accuracy, the proposed method surpasses the other methods. Its position on the graph serves as a visual confirmation of its superiority. When compared to existing techniques, this graphical representation reinforces the idea that the proposed method is not only statistically better but also consistent.

In conclusion, Table 3 and Figure 17 show that the anticipated method is a highly accurate and superior approach to brain tumor detection. These results are not only statistically significant but also visually obvious, demonstrating the efficacy of the proposed method and its potential to advance the field of medical image analysis.

Table 4 provides a thorough assessment of the projected brain tumor detection model, HSO+RNN, with emphasis on the specificity and sensitivity metrics. In medical image analysis, these metrics are critical for determining a model's ability to accurately identify true negatives and positives. Table 4 clearly shows that the HSO+CNN model outperforms earlier methods, such as the improved residual network, chronological artificial vulnerability optimization (CAVO), and i-YOLOV5. The HSO+RNN model consistently achieved higher specificity and sensitivity values, demonstrating its superior ability to detect the presence or absence of brain tumors.

Furthermore, Figure 19 supplements the statistical findings by depicting the comparative performances of the various methods. This plot emphasizes the dominance of the HSO+CNN model, placing it at the top of the graph and visually demonstrating its advanced capabilities in brain tumor detection. Table 4 and Figure 18 show that the proposed model is superior, both statistically and visually, making it a promising candidate for advancing the field of medical image analysis and brain tumor detection.

Table 3. Accuracy performance evaluation.

Techniques used	Accuracy (%)
Recurrent networks and CNN (ConvNets) [22]	98.3
Machine learning [23]	95.83
Texture-based and statistical features [24]	97.87
Modified two-step dragonfly mechanism system [25]	98.20
2D CNN [30]	96.47
Autoencoder [30]	95.63
Proposed method	99.13

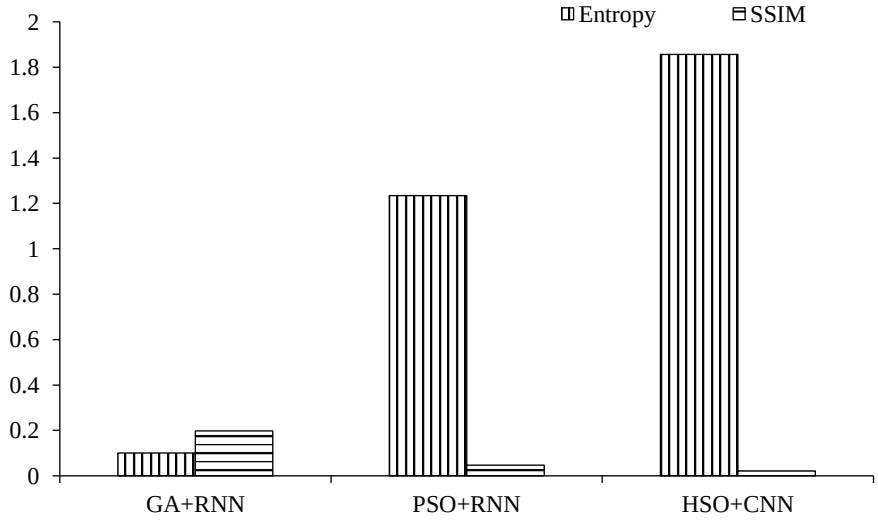

Figure 17. Entropy and SSIM graphical representation for GA and PSO algorithms with RNN.

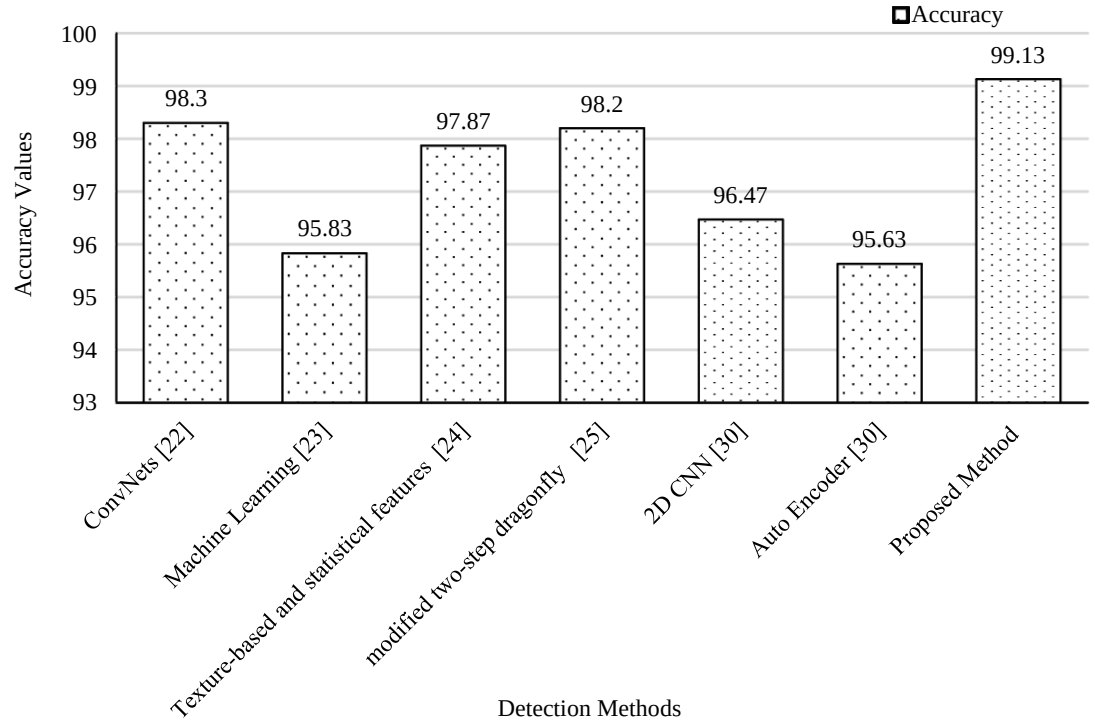

Figure 18. Comparative plot for accuracy in brain tumor detection.

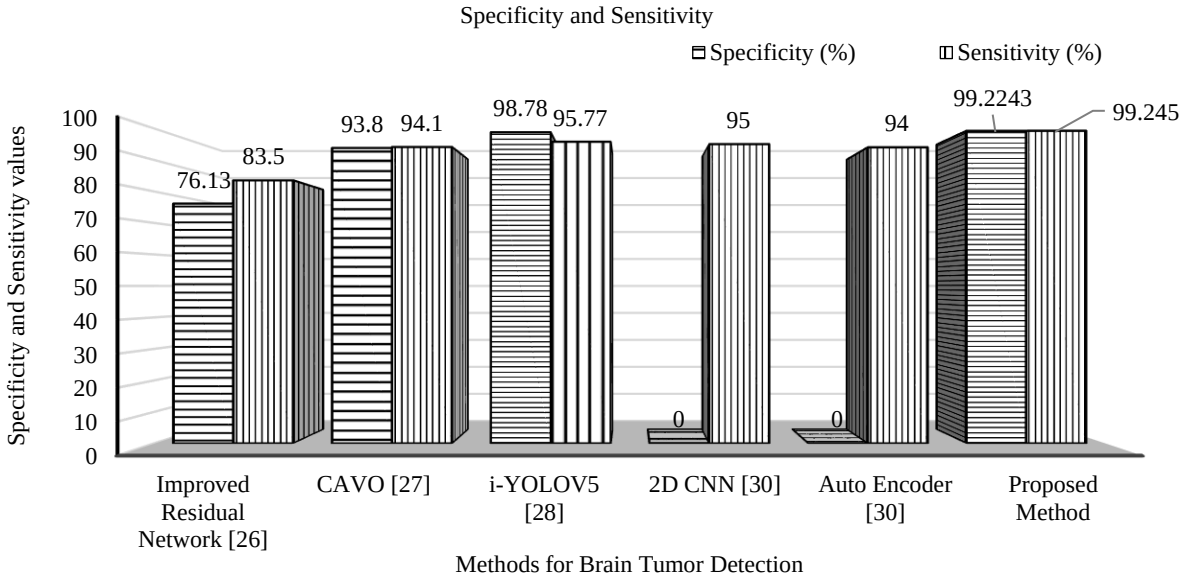

Figure 19. Comparative plot for specificity and sensitivity in brain tumor detection.

Table 4. Performance evaluation for specificity and sensitivity in brain tumor detection.

Year	Techniques used	Specificity (%)	Sensitivity (%)
2023	Improved Residual Network [26]	76.13	83.5
2023	Chronological Artificial Vultures Optimization (CAVO) [27]	93.8	94.1
2022	*i*-YOLOV5 [28]	98.78	95.77
2023	2D CNN [30]	--	95
2023	Auto Encoder [30]	--	94
2023	Proposed Method	99.2243	99.245

CONCLUSION AND FUTURE SCOPE

Finally, our research delves into the multifaceted realm of automatic segmentation of MRI brain images, a domain fraught with difficulties owing to the intricate brain structure. In this context, we combined the power of the GA with RNN and PSO with RNN, demonstrating their exceptional ability to accurately partition the tumor region. The statistical parameters highlight their distinct strengths even more: GA+RNN outperforms PSO+RNN in MSE and PSNR, whereas PSO+RNN excels in Entropy and Structural Similarity Index (SSIM). These findings highlight the synergistic potential of both approaches, laying the groundwork for their effective coexistence in the field of brain tumor detection. The proposed methodology, which combines HSO and CNN, has proven to be extremely effective in detecting and classifying brain tumors from MRI and CT images with a 99.13% accuracy rate. This integration not only improves diagnostic accuracy but also reduces reliance on radiologists' expertise and promises better patient care. Subsequent research will seek to reduce computational complexity and investigate alternative optimization algorithms for feature extraction to ultimately improve the efficiency of our proposed system. Although our research has already produced impressive results, future research will concentrate on fine-tuning specific parameters to determine the best algorithmic choice.

Supplementary Materials

Not applicable.

Funding

The authors received no funding for this research.

Acknowledgment

None.

Author Contributions

Shaik Karimullah contributed to the study's conception, design, data collection, and software development. Fahimuddin Shaik was responsible for the analysis and interpretation of the results, as well as the preparation of the draft manuscript and supervision of the project. Both authors reviewed the results and approved the final version of the manuscript.

Availability of Data and Materials

The data and materials are accessible and can be made available upon genuine request from the corresponding author.

Conflicts of Interest

The authors declare that they have no conflict of interest regarding this study.

REFERENCES

1. Sung H, Ferlay J, Siegel RL, Laversanne M, Soerjomataram I, Jemal A, et al. Global cancer statistics 2020: GLOBOCAN estimates of incidence and mortality worldwide for 36 cancers in 185 countries. CA Cancer J Clin. 2021;71:209-49. DOI: 10.3322/caac.21660.
2. McNeill KA. Epidemiology of brain tumors. Neurol Clin. 2016;34:981-98. DOI: 10.1016/j.ncl.2016.06.014.
3. Johnson KJ, Cullen J, Barnholtz-Sloan JS, Ostrom QT, Langer CE, Turner MC, et al. Childhood brain tumor epidemiology: A brain tumor epidemiology consortium review. Cancer Epidemiol Biomarkers Prev. 2014;23:2716-36. DOI: 10.1158/1055-9965.EPI-14-0207.
4. Khambhata K. Multiclass classification of brain tumor in MR images. Int J Innov Res Comput Commun Eng. 2016;4:8982-92.
5. Madhukumar S, Santhiyakumari N. Evaluation of k-Means and fuzzy C-means segmentation on MR images of brain. Egypt J Radiol Nucl Med. 2015;46:475-9. DOI: 10.1016/j.ejrnm.2015.02.008.

6. Das V, Rajan J. Techniques for MRI brain tumor detection: A survey. Int J Res Comput Appl Inf Technol. 2016;4:53-6.
7. Karimullah S, Vishnuvardhan D. Experimental analysis of optimization techniques for placement and routing in Asic design. In: ICDSMLA 2019. Proc 1st Int Conf Data Sci Mach Learn Appl. Singapore: Springer; 2020. p. 908-17. DOI: 10.1007/978-981-15-1420-3_99.
8. Işın A, Direkoğlu C, Şah M. Review of MRI-based brain tumor image segmentation using deep learning methods. Procedia Comput Sci. 2016;102:317-24. DOI: 10.1016/j.procs.2016.09.407.
9. Kong Y, Deng Y, Dai Q. Discriminative clustering and feature selection for brain MRI segmentation. IEEE Signal Process Lett. 2015;22:573-7. DOI: 10.1109/LSP.2014.2364612.
10. Chen H, Zou Q, Wang Q. Clinical manifestations of ultrasonic virtual reality in the diagnosis and treatment of cardiovascular diseases. J Healthc Eng. 2021;2021:1746945. DOI: 10.1155/2021/1746945.
11. Avşar E, Salçin K. Detection and classification of brain tumours from MRI images using faster R-CNN. Teh Glasnik. 2019;13:337-42. DOI: 10.31803/tg-20190712095507.
12. Aslam A, Khan E, Beg MMS. Improved edge detection algorithm for brain tumor segmentation. Procedia Comput Sci. 2015;58:430-7. DOI: 10.1016/j.procs.2015.08.057.
13. Bauer S. Medical image analysis and image-based modeling for brain tumor studies [PhD dissertation]. Universitä˙T Bern; 2013.
14. Shaik F, Sharma AK, Ahmed SM. Detection and analysis of diabetic myonecrosis using an improved hybrid image processing model. In: Proc 2nd Int Conf Adv Electr Electron Inf Commun Bio-Informatics (AEEICB). IEEE Publications; 2016. p. 314-7. DOI: 10.1109/AEEICB.2016.7538298.
15. Saba T, Mohamed AS, El-Affendi M, Amin J, Sharif M. Brain tumor detection using fusion of hand crafted and deep learning features. Cogn Syst Res. 2020;59:221-30. DOI: 10.1016/j.cogsys.2019.09.007.
16. Karimullah S, Vishnuvardhan D, Arif M, Gunjan VK, Shaik F, Siddiquee KN. An improved harmony search approach for block placement for VLSI design automation. Wireless Commun Mob Comput. 2022;2022:1-10. DOI: 10.1155/2022/3016709.
17. Gordon R, Bender R, Herman GT. Algebraic reconstruction techniques (ART) for three-dimensional electron microscopy and X-ray photography. J Theor Biol. 1970;29:471-81. DOI: 10.1016/0022-5193(70)90109-8.
18. Mishra PK, Satapathy SC, Rout M. Segmentation of MRI brain tumor image using optimization based deep convolutional neural networks (DCNN). Open Comput Sci. 2021;11:380-90. DOI: 10.1515/comp-2020-0166.
19. Irmak E. Multi-classification of brain tumor MRI images using deep convolutional neural network with fully optimized framework. Iran J Sci Technol Trans Electr Eng. 2021;45:1015-36. DOI: 10.1007/s40998-021-00426-9.
20. Datta S, Chakraborty M. Brain tumor detection from preprocessed MR images using segmentation techniques. In: IJCA Special Issue on 2nd National Conference Computing, Communication and Sensor Network; 2011: 1–5.
21. Karimullah S, Vishnuvardhan D. Pin density technique for congestion estimation and reduction of optimized design during placement and routing. Appl Nanosci. 2023;13:1819-28. DOI: 10.1007/s13204-021-02173-z.
22. Sharma AK, Tiwari S, Aggarwal G, Goenka N, Kumar A, Chakrabarti P, et al. Dermatologist-level classification of skin cancer using cascaded ensembling of convolutional neural network and handcrafted features based deep neural network. IEEE Access. 2022;10:17920-32. DOI: 10.1109/ACCESS.2022.3149824.
23. Zhang J, Zhou H, Niu Y, Lv J, Chen J, Cheng Y. CNN and multi-feature extraction based denoising of CT images. Biomed Signal Process Control. 2021;67:102545. DOI: 10.1016/j.bspc.2021.102545.

24. Hossain T, Shishir FS, Ashraf M, Al Nasim MA, Shah FM. Brain tumor detection using convolutional neural network. In: 2019 1st International Conference on Advances in Science, Engineering and Robotics Technology (ICASERT). IEEE Publications; 2019. p. 1-6. DOI: 10.1109/ICASERT.2019.8934561.
25. Khalil HA, Darwish S, Ibrahim YM, Hassan OF. 3D-MRI brain tumor detection model using modified version of level set segmentation based on dragonfly algorithm. Symmetry. 2020;12:1256. DOI: 10.3390/sym12081256.
26. Aggarwal M, Tiwari AK, Sarathi MP, Bijalwan A. An early detection and segmentation of brain tumor using deep neural network. BMC Med Inform Decis Mak. 2023;23:78. DOI: 10.1186/s12911-023-02174-8.
27. Geetha M, Prasanna Lakshmi K, Arumugam SR, Sandhya N. Conditional random field-recurrent neural network segmentation with optimized deep learning for brain tumour classification using magnetic resonance imaging. Imaging Sci J. 2023;71(3):199-220. DOI: 10.1080/13682199. 2023.2178611.
28. Arunachalam S, Sethumathavan G. An effective tumor detection in MR brain images based on deep CNN approach: I- YOLOV5. Appl Artif Intell. 2022;36:2151180. DOI: 10.1080/08839514. 2022.2151180.
29. Menze BH, Jakab A, Bauer S, Kalpathy-Cramer J, Farahani K, Kirby J, et al. The Multimodal Brain Tumor Image Segmentation Benchmark (BRATS). IEEE Trans Med Imaging. 2015;34:1993-2024. DOI: 10.1109/TMI.2014.2377694.
30. Saeedi S, Rezayi S, Keshavarz H, Niakan Kalhori SR. MRI-based brain tumor detection using convolutional deep learning methods and chosen machine learning techniques. BMC Med Inform Decis Mak. 2023;23:16. DOI: 10.1186/s12911-023-02114-6.
31. Rezayi S, Mohammadzadeh N, Bouraghi H, Saeedi S, Mohammadpour A. Timely diagnosis of acute lymphoblastic leukemia using artificial intelligence-oriented deep learning methods. Comput Intell Neurosci. 2021;2021:5478157. DOI: 10.1155/2021/5478157.

